Plant Science 253 (2016) 21–30

Contents lists available at ScienceDirect

Plant Science

journal homepage: www.elsevier.com/locate/plantsci

An ABC transporter, OsABCG26, is required for anther cuticle and pollen exine formation and pollen-pistil interactions in rice

Zhenyi Chang[a,e,1], Zhufeng Chen[a,1], Wei Yan[c,1], Gang Xie[a], Jiawei Lu[a], Na Wang[a], Qiqing Lu[a], Nan Yao[d], Guangzhe Yang[b], Jixing Xia[b,**], Xiaoyan Tang[a,e,*]

[a] Shenzhen Institute of Molecular Crop Design, Shenzhen 518107, China
[b] State Key Laboratory of Conservation and Utilization of Subtropical Agro-bioresources, College of Life Science and Technology, Guangxi University, Nanning 530005, China
[c] School of Life Sciences, Capital Normal University, Beijing 100048, China
[d] School of Life Sciences, Sun Yat-Sen University, Guangzhou 510275, China
[e] Guangdong Key Lab of Biotechnology for Plant Development, College of Life Sciences, South China Normal University, Guangzhou 510631, China

ARTICLE INFO

Article history:
Received 5 April 2016
Received in revised form
15 September 2016
Accepted 16 September 2016
Available online 21 September 2016

Keywords:
ABC transporter
Male sterility
Pollen exine
Anther cuticle
Pollen tube growth

ABSTRACT

Wax, cutin and sporopollenin are essential components for the formation of the anther cuticle and the pollen exine, respectively. Their lipid precursors are synthesized by secretory tapetal cells and transported to the anther and microspore surface for deposition. However, the molecular mechanisms involved in the formation of the anther cuticle and pollen exine are poorly understood in rice. Here, we characterized a rice male sterile mutant *osabcg26*. Molecular cloning and sequence analysis revealed a point mutation in the gene encoding an ATP binding cassette transporter G26 (OsABCG26). *OsABCG26* was specifically expressed in the anther and pistil. Cytological analysis revealed defects in tapetal cells, lipidic Ubisch bodies, pollen exine, and anther cuticle in the *osabcg26* mutant. Expression of some key genes involved in lipid metabolism and transport, such as *UDT1*, *WDA1*, *CYP704B2*, *OsABCG15*, *OsC4* and *OsC6*, was significantly altered in *osabcg26* anther, possibly due to a disturbance in the homeostasis of anther lipid metabolism and transport. Additionally, wild-type pollen tubes showed a growth defect in *osabcg26* pistils, leading to low seed setting in *osabcg26* cross-pollinated with the wild-type pollen. These results indicated that *OsABCG26* plays an important role in anther cuticle and pollen exine formation and pollen-pistil interactions in rice.

1. Introduction

Male reproductive development in flowering plants is a complex biological process from the formation of the anther primordium, to the production of mature pollen within the anther and dehiscence [1]. Anther and pollen development is a prerequisite for male reproductive success. The anther consists of four distinct layers of cells, from exterior to interior the epidermis, the endothecium, the middle layer, and the tapetum [1]. At the center of each anther lobe, microspores are produced, differentiated, and developed into mature pollen grains. The anther and pollen are respectively covered by anther cuticle and pollen exine, which have a protective role against environmental and biological stresses during reproductive development [2].

The anther cuticle consists of cutin and wax [2–4]. Cutin is a mixture of lipophilic biopolymers comprised of hydroxylated and epoxy C16 and C18 fatty acids, while cuticular wax is a biopolymer containing a mixture of alcohols, ketones, aldehydes, alkanes, and long-chain fatty acids [2–5]. The pollen exine is composed of a rigid material called sporopollenin, which is made up of complex biopolymers derived mainly from phenolics and aliphatic derivatives [2,6,7]. The tapetum is considered to act as a supplier of sporopollenin and anther cuticle precursors [8,9]. By analyzing male sterile mutants defective in the production of the anther cuticle and pollen exine, a number of different proteins, such as enzymes for lipid synthesis and modification, lipid transfer proteins (LTPs), ABCG transporters, and transcription factors, have been identified [2,9,10]. They are required for the synthesis and deposition of sporopollenin and cuticle in *Arabidopsis* and rice. For

* Corresponding author at: Shenzhen Institute of Molecular Crop Design, Xinjianxing Industrial Park, Fengxin Street, Guangming New District, Shenzhen, 518107, China.
** Corresponding author.
E-mail addresses: xiajx@gxu.edu.cn (J. Xia), txy@frontier-ag.com (X. Tang).
[1] These authors contributed equally to this work.

http://dx.doi.org/10.1016/j.plantsci.2016.09.006

example, *MS2*, *ACOS5*, *PKSA*, *PKSB*, *TKPR1*, *CYP703A2*, and *CYP704B1* encode enzymes functioning in the synthesis of sporopollenin and cutin in *Arabidopsis* [2,9,10]. *AtABCG11*, *AtABCG12* and *AtABCG26* in *Arabidopsis* encode plasma membrane-localized ABC transporters acting in lipidic precursor export from the tapetum [11–16]. Recently, *OsABCG15*, the homolog of *AtABCG26*, was reported to transport lipidic precursors from tapetal cells to the anther cuticle and pollen wall in rice [17–20]. WDA1, CYP704B2, DPW and CYP703A3 were identified as enzymes involved in the synthesis of sporopollenin in rice [21–24]. OsC4 and OsC6 were considered to be LTPs related to lipid trafficking during rice anther and pollen exine formation [25]. Transcription factors such as UDT1, TDR and GAMYB were proposed to be major regulators in rice pollen development [26–28]. Despite these recent progresses, our knowledge of the mechanism underlying the lipid transport from the tapetum is still limited.

Very recently, *OsABCG26* was reported to cooperate with *OsABCG15* functioning in the formation of anther cuticle and pollen exine by the transport of lipidic precursors in rice [29]. Here, we reported the isolation and characterization of an allelic mutant of *OsABCG26* caused by a point mutation. Similar to what was reported, we found that *OsABCG26* was involved in the formation of anther cuticle and pollen exine by regulating lipid transport from the tapetum. More interestingly, we found that wild-type pollen germinated on the mutant stigma normally, but most of the pollen tubes ceased growth in the mutant pistil and failed to reach the micropyle, suggesting that *OsABCG26* plays an important role in pollen-pistil interaction by affecting pollen tube growth in the pistil.

2. Materials and methods

2.1. Plant materials and growth conditions

Mutants *osabcg26* and *osabcg15* were derived from the *indica* cv. Huanghuazhan (HHZ) by ethyl methanesulfonate (EMS) mutagenesis [30]. HHZ was used as the wild-type control. All the plants (*Oryza sativa*) were grown in the paddy field of Shenzhen, China, under natural conditions with regular care.

2.2. Characterization of the mutant phenotype

To analyze pollen fertility, pollen grains at mature stage were stained with 1% I_2-KI solution and photographed using Nikon AZ100 microscope.

Spikelets at different developmental stages were collected and embedded as described previously with some modifications [27]. Briefly, spikelets were pre-fixed with 2.5% glutaraldehyde and 2% paraformaldehyde in 0.1 M PBS (pH 7.0) at 4 °C for 24 h, and post-fixed with 1% osmium tetroxide in 0.1 M PBS (pH 7.0) for 1–2 h. Subsequently, samples were dehydrated with ethanol and embedded in SPI-PON 812 resin (SPI-CHEM). Semi-thin sections (1 μm) were obtained on an ultramicrotome (Leica EM-UC6) using a diamond knife (DiATOME) and stained with 0.5% toluidine blue. Ultra-thin sections (100 nm) were double stained with uranyl acetate and lead citrate solution, and examined with a transmission electron microscope (JEOL, JEM1400) at an accelerating voltage of 120 kV.

For scanning electron microscopy, anthers were fixed in FAA solution (38% formaldehyde 5 mL, acetic acid 5 mL, 50% alcohol 90 mL). Following ethanol dehydration, samples were processed for critical point drying and gold coated [18]. Finally, samples were observed under scanning electron microscope (Hitachi S-3400N) with an acceleration voltage of 10 kV.

2.3. Mutant gene cloning and HRM analysis

The *osabcg26* mutant was backcrossed with wild-type HHZ, and the resulted F1 was further selfed to generate the F2 population. Thirty male sterile plants in F2 population were randomly selected for DNA extraction, and equal amount of DNA was pooled and sequenced to 43x of genome coverage using the Illumina Hiseq 2000 platform. The data were subjected to computational analysis for identification of the mutant gene as described [30]. Co-segregation of the candidate mutation with the male sterile phenotype in F2 population was analyzed using high resolution melting (HRM) analysis [31]. Primer set OsABCG26-P1 used for HRM analysis is listed in Table S1.

2.4. Plasmid construction and rice transformation

The 8.0 kb HHZ genomic DNA fragment for *OsABCG26*, including a 2.0 kb upstream region, 5.3 kb coding region, and 0.7 kb downstream region, was PCR-amplified with primer set OsABCG26-P2. The PCR products were digested with *Kpn*I and *BamH*I, and cloned into the binary vector pCAMBIA1300 to generate construct pCAMBIA1300-*OsABCG26* for mutant complementation. The 2.0 kb upstream region of *OsABCG26* was PCR-amplified with primer set OsABCG26-P3, and cloned into binary vector pHPG between *Kpn*I and *Sal*I, to yield $OsABCG26_{pro}$:*GUS* for promoter analysis. Both constructs were sequence-confirmed before transformation. Constructs were introduced into *Agrobacterium tumerfaciens* AGL10 strain and transformed into rice calli. pCAMBIA1300-*OsABCG26* was introduced into offspring of *osabcg26* heterozygote plants. $OsABCG26_{pro}$:*GUS* was introduced into *japonica* cv. Zhonghua11. The positive transgenic lines were determined by PCR with primer set HPTII. To identify the background genotype of pCAMBIA1300-*OsABCG26* transgenic plants, specific genomic fragment covering the mutant site of *osabcg26* was amplified using primer set OsABCG26-P4, and the product was diluted 1000 times and further subjected to HRM analysis with primers OsABCG26-P1. Primers used are listed in Table S1.

2.5. qRT-PCR assay

Rice tissues were collected at the reproductive stage. The stages of anthers were classified as previously described [1]. Total RNA was extracted using Trizol reagent (Invitrogen, Carlsbad, CA, USA) and then reverse-transcribed with PrimeScript™ RT reagent Kit with gDNA Eraser (Takara, Dalian, China), according to the manufacturer protocols. qRT-PCR was performed with an Applied Biosystems 7500 Real-Time PCR System using SYBR Premix Ex Taq™ II (Takara, Dalian, China), following the manufacturer instructions. Each experiment was biologically repeated three times, each with three replicates. *OsACTIN1* was used as the normalized reference. The relative expression levels were measured using the $2^{-\Delta\Delta Ct}$ analysis method. Primer sequences used are listed in Table S1.

2.6. GUS staining

Histochemical GUS assay was performed as described [28], except for the addition of 0.1% (v/v) Triton X-100 to the staining solution. After staining, samples were cleared with 70% (v/v) ethanol and photographed using Nikon AZ100 microscope.

2.7. Histological analyses of ovule

Wild-type and *osabcg26* spikelets at different developmental stages were fixed with FAA solution, dehydrated with an ethanol series followed by a xylene series, and then embedded in Paraplast Plus (Sigma, St. Louis, MO), as described [32]. Samples were

sectioned to 8 μm thick, stained with 0.5% toluidine blue, and photographed using Nikon AZ100 microscope. Whole-mount stain-clearing laser scanning confocal microscopy (WCLSM) analysis of mature embryo sacs was performed as previously described [33].

2.8. Pollination, pollen germination and pollen tube growth assays

Wild-type HHZ was self-pollinated, while *osabcg15* and *osabcg26* mutants were cross-pollinated with the wild-type HHZ pollen manually. Cross-pollination experiment was repeated three times, each group with 3–6 plants. Pollen germination and pollen tube growth were examined by aniline blue staining as described previously [34]. Briefly, the pistils were excised at the time point of 30 min, 2 h, 4 h, 6 h, and 8 h after pollination, fixed in 3:1 ethanol: acetic acid solution for 30 min, softened in 1 M KOH for 30 min at 56 °C, and then stained with 0.1% (w/v) aniline blue in 50 mM KPO_4 buffer (pH 8.5) for 2 h at room temperature. The samples were visualized by Nikon AZ100 microscope. The seed setting rate was scored at 20 d after pollination.

2.9. CRISPR/Cas9-mediated mutation

The CRISPR/Cas9 genome targeting system was used to create mutant alleles of *OsABCG26* in *japonica* cv. Wuyunjing7. The pCRISPR-*OsABCG26* plasmid, with two target sites specifically for *OsABCG26*, was constructed as previously described [35]. One target site was AGGGCACAATCGTCGAGATG (on the second exon of *OsABCG26*), the other target site was CGCTTGTATCTCCTTTCAGG (on the third exon of *OsABCG26*). The construct was introduced into *Agrobacterium tumefaciens* strain AGL0 and transformed into rice Wuyunjing7. The genomic DNA of T0 transgenic lines was subjected to HRM analysis with specific primer sets, OsABCG26-P6 and OsABCG26-P7, respectively, followed by amplification and sequencing using primer OsABCG26-P8.

3. Results

3.1. Isolation and phenotypic observation of the male sterile mutant

A male sterile mutant was isolated from a HHZ mutant library generated by EMS treatment. The mutant exhibited normal vegetative and floral development (Fig. 1A and B), but had short whitish anthers with no pollen grain (Fig. 1C–F). When the mutant was backcrossed with wild-type HHZ, all of the F1 plants were fertile, and the F2 population displayed an approximate 3:1 segregation of fertile to male sterile (233:85, $\chi^2 = 1.13$, $0.05 < P < 0.10$), indicating that the male sterile phenotype was controlled by a single recessive gene. We designated this mutant *osabcg26* because a point mutation was revealed in the gene *OsABCG26* (see below).

3.2. Anatomic characterization of osabcg26 anthers

To investigate the cellular defects in *osabcg26*, we carried out transverse sections of anthers of wild-type HHZ and the *osabcg26* mutant at different developmental stages. Rice anther development is divided into 14 stages from the formation of stamen primordium to the release of mature pollen during anther dehiscence [1]. By stage 6, the wild-type anther primordia differentiate to a concentric structure, with pollen mother cells (PMCs) in the locule surrounded by a four-layered anther wall, from surface to interior the epidermis, endothecium, middle layer, and tapetum. The PMC subsequently undergoes meiosis and generates a tetrad by the end of stage 8b. Meanwhile, tapetal cells initiate programmed cell death, and the middle layer becomes nearly invisible [1].

No clear defects were observed in *osabcg26* mutant before stage 8a when microspores finish meiosis I forming dyads (Fig. 2A–D). However, clear differences were observed between the wild-type and *osabcg26* mutant after stage 8b. The middle layer vanished in the wild-type anther at stage 8b but persisted in *osabcg26* till stage 11 (Fig. 2E–N). Globular microspores were released from tetrads by stage 9 in the wild-type, but microspores in the mutant exhibited an irregular shape (Fig. 2G–H). At stage 10, the wild-type microspores were spherical containing a large vacuole, but the mutant microspores collapsed (Fig. 2I–J). Subsequently, the wild-type microspores underwent two rounds of cell division forming mature pollen grains, but the mutant anther contained the expanded middle layer and endothecium, and exhibited empty and shriveled locules lacking microspores (Fig. 2K–N).

To obtain more details of the defects in *osabcg26* anther, transmission electron microscopy (TEM) analysis was performed for anthers at stages 8b to 12. The abnormal persistence of an expanded middle layer in *osabcg26* mutant was confirmed (Fig. 3A–D, I–J and M–N). From stage 8b to stage 10, the wild-type tapetum underwent programmed cell death and was highly condensed, but the mutant tapetum was less condensed (Fig. 3A–F and I–L). At stage 9, numerous primary Ubisch bodies, which are thought to export sporopollenin precursors from the tapetum to the microspore, were formed at the peripheral side of the tapetum in the wild-type anther (Fig. 3E), and a primary exine structure was formed on the microspore (Fig. 3G). In *osabcg26*, however, no primary Ubisch bodies were observed, and the primary pollen exine was thinner (Fig. 3F and H). The Ubisch bodies further enlarged, and the exine thickened and formed distinct structure in the wild-type at stage 10 and afterwards (Fig. 3K and M). Whereas in *osabcg26*, Ubisch bodies were not formed, the microspore exine was thinner without distinct structure (Fig. 3L and N), and the microspores eventually collapsed in the mutant locule (Fig. 3N). In addition, defects in anther epidermis were also observed in the mutant. Before stage 10, the cuticles of the wild-type and mutant anther epidermis were smooth and thin. Starting from stage 11, the cuticle of the wild-type anther was thickened with extrusive finger-like structures formed (Fig. 3O), but the cuticle of *osabcg26* anther was still smooth and thin (Fig. 3P).

To confirm the defective formation of the mutant anther cuticle, we further examined the anther epidermis using scanning electron microscope (SEM). In agreement with the TEM results, the cuticle formed well-ordered and thickened nano-ridges in the wild-type anther epidermis from stage 11, but the *osabcg26* anther showed a smooth outer surface (Fig. 4C–H). Moreover, the anther of *osabcg26* was also shorter and smaller (Fig. 4A and B).

3.3. Cloning of the osabcg26 gene

A next generation sequencing method was used to identify the mutant gene causing male sterility in the *osabcg26* mutant [30]. Total DNA from 30 F2 progeny with the mutant phenotype were bulked and then sequenced to about 43× of genome coverage on Illumina Hiseq 2000 platform, resulting in 177,165,334 clean reads (101 bp), of which, 73.59% (137,464,723) were aligned to the Nipponbare reference sequence released by MSU (v7). Re-sequencing data of other mutants derived from the same HHZ mutant library were utilized as reference during the analysis (W.Y. and X.T., unpublished results), and 867 SNPs were identified to be specific to the *osabcg26* mutant. The candidate region harboring the causal mutation was located between 18.69 and 19.27 Mb on chromosome 10 (Supplementary Fig. S1). SNPs within the candidate region with high SNP index and ED score were evaluated, and those inducing an amino acid substitution or located at an exon-intron splicing site were considered candidates. A G-to-A SNP (Chr10: 18,789,017) with the highest scores was identified at the 8th exon-intron splicing site of gene *Os10g0494300* encoding an

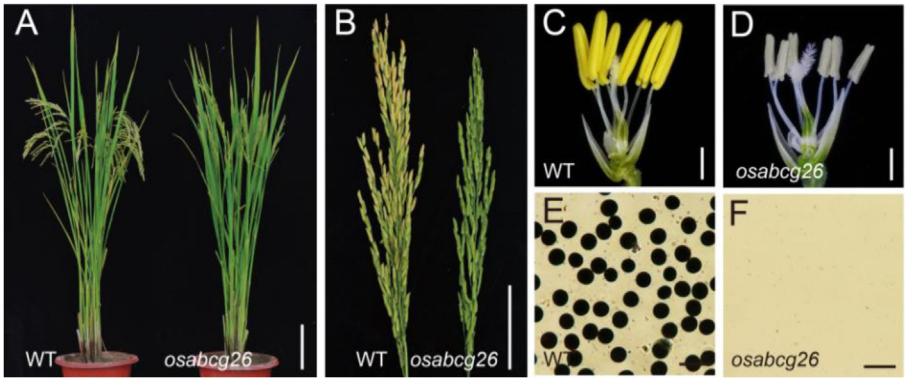

Fig. 1. Phenotype of *osabcg26*. (A) Wild-type (WT) and *osabcg26* after heading. (B) WT and *osabcg26* seed setting. (C, D) Spikelets of WT and *osabcg26* with the palea and lemma removed. (E, F) Pollen grains of WT and *osabcg26* with I_2-KI staining. Scale bars: A, 10 cm; B, 5 cm; C, 1 mm; D, 100 μm.

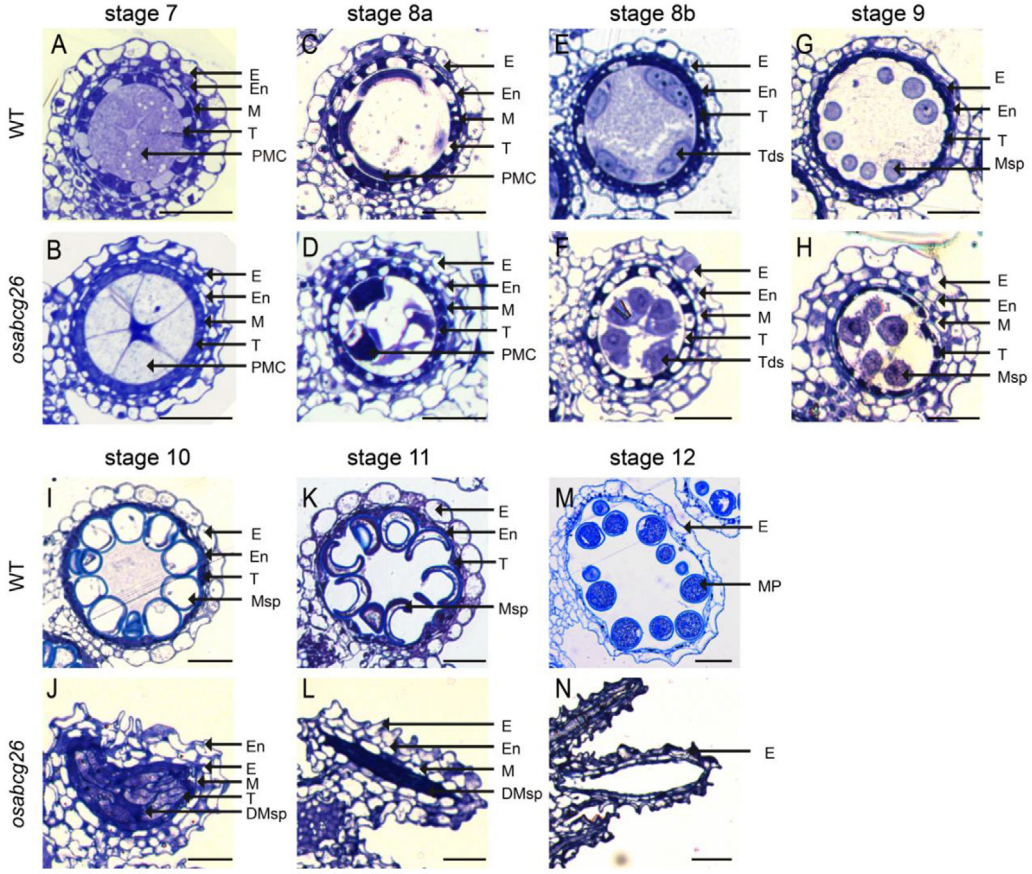

Fig. 2. Transverse sections of anther development in wild-type (WT) and *osabcg26* from stage 7 to stage 12. Wild-type anthers are shown in A, C, E, G, I, K, M, and *osabcg26* anthers are shown in B, D, F, H, J, L, N. DMsp, degenerated microspores; E, epidermis; En, endothecium; M, middle layer; MP, mature pollen; Msp, microspores; PMC, pollen mother cell; T, tapetal layer; Tds, tetrads. Bars = 20 μm.

ABC transporter designated as OsABCG26 (Fig. 5A). The mutation alters the exon-intron splicing of *Os10g0494300*, producing a C-terminal truncation (Fig. 5B). High resolution melting (HRM) assay was performed to verify the linkage between the candidate SNP and mutant phenotype using individuals from the F2 population. All 41 male sterile plants carried the mutant SNP in *Os10g0494300*, whereas fertile plants displayed 2:1 ratio of the heterozygous to homozygous wild-type genotypes (32:19), demonstrating that the SNP in *Os10g0494300* co-segregated with the male sterile phenotype.

To confirm the mutation, a complementation experiment was performed by introducing a construct of an 8.0-kb genomic DNA fragment containing the promoter and coding sequence of *OsABCG26* into the *osabcg26* mutant plant. The pollen fertility of transgenic plants was restored to normal (Supplementary Fig. S2). These results demonstrated that the male sterile phenotype was caused by the point mutation in *OsABCG26*.

OsABCG26 consists of 10exons and 9 introns, encoding a protein of 726 amino acids belonging to the G subfamily of rice ABC transporters. A database search using the OsABCG26 amino acid sequence as a query revealed its close homologs in *Arabidopsis* and rice. The closest homolog of OsABCG26 in *Arabidopsis* is AtABCG11, a known fertility-related protein (Fig. 5C) [13]. OsABCG26 also shows high similarity to three other known fertility-related pro-

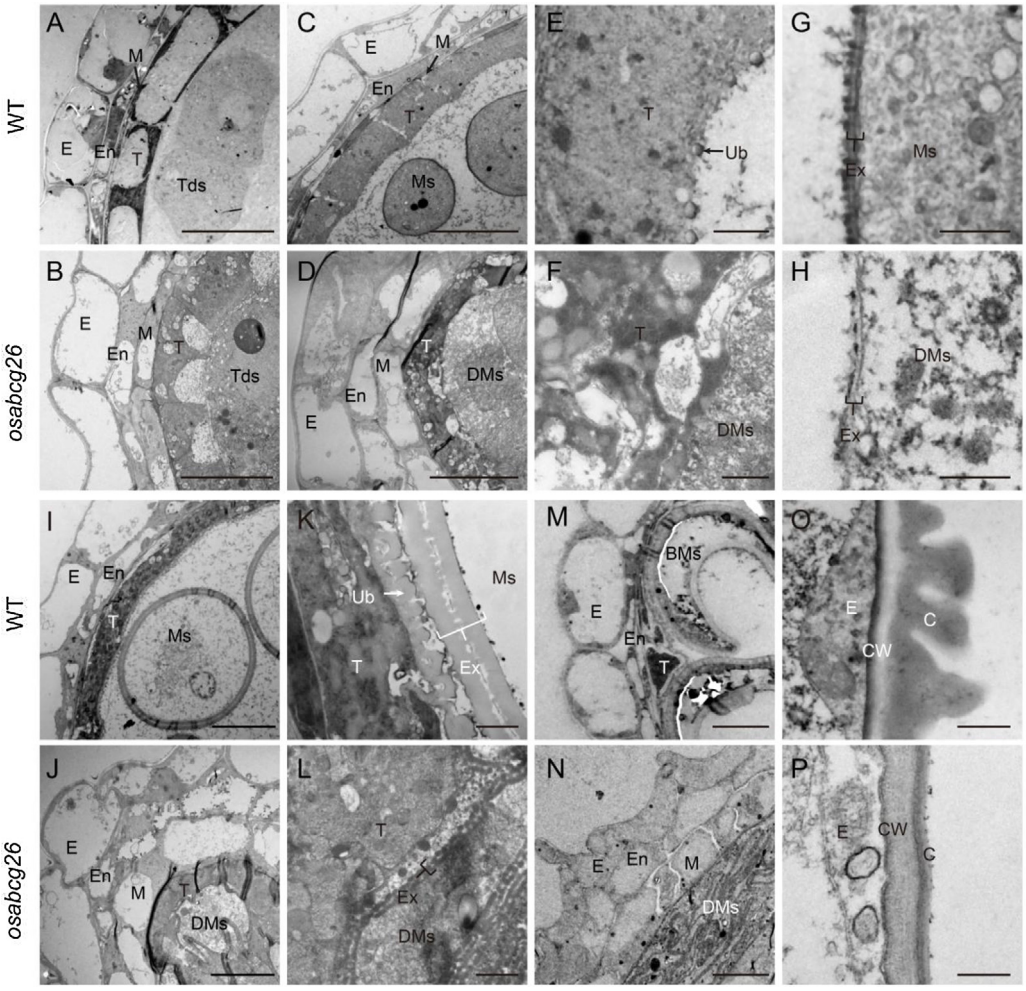

Fig. 3. TEM analysis of the wild-type (WT) and *osabcg26* anther sections from stages 8b–12. (A–B), stage 8b; (C–H), stage 9; (I–L), stage 10; (M–N), stage 11; (O–P), stage 12. BMs, Binuclear microspores; C, cuticle; CW, cell wall; DMs, degenerated microspore; E, epidermis; En, endothecium; Ex, exine; M, middle layer; Ms, microspores; T, tapetal layer; Ub, Ubisch body. Scale bars: A–D, I–J, M and N, 10 μm; E, F, K and L, 1 μm; G, H, O and P, 500 nm.

teins, AtABCG12, AtABCG26, and OsABCG15 (Fig. 5C) [14–20], suggesting that the functions of these ABCG proteins were conserved during evolution.

3.4. Expression pattern of OsABCG26

The expression levels of *OsABCG26* in various rice organs, including root, stem, leaf, glume, palea, lemma, anthers from stage 6 to 12, and pistil, were determined using quantitative reverse transcription PCR (qRT-PCR). *OsABCG26* was specifically expressed in the anther and pistil (Fig. 6A). The expression of *OsABCG26* was detected in anthers beginning at stage 6, and up-regulated till stage 9, and then declined (Fig. 6A). The tissue-specific expression was confirmed in *OsABCG26* promoter-GUS transgenic plants, which showed GUS staining in anther and pistil (Fig. 6B). These results suggested that *OsABCG26* may function specifically in rice reproductive development.

3.5. Expression analysis of genes involved in anther lipid metabolism and transport in osabcg26

To investigate the impact of *osabcg26* mutation on the transcriptional levels of known genes related to lipid metabolism and transport during anther development, we compared the expression levels of nine genes (*GAMYB*, TDR, *UDT1*, *WDA1*, *CYP704B2*, *OsABCG15*, *OsABCG26*, *OsC4* and *OsC6*) between the wild-type and mutant anthers [17–28]. Among the three regulatory genes, the expression levels of *GAMYB* and *TDR* were similar between the wild-type and *osabcg26*, while the expression level of *UDT1* was significantly reduced in *osabcg26* (Fig. 7). The expression levels of genes for lipid biosynthesis and transport, including *WDA1*, *CYP704B2*, and *OsABCG15*, were decreased in *osabcg26* at stages 8 to 9, and then up-regulated at stage 10 (Fig. 7). In addition, the expression levels of both *OsC4* and *OsC6* involved in lipid trafficking were dramatically decreased in *osabcg26* (Fig. 7). These results suggested that *OsABCG26* plays an important role in maintaining lipid metabolism homeostasis in anther.

3.6. Functional analysis of OsABCG26 in the pistil

OsABCG26 exhibited substantial expression in the pistil (Fig. 6). Therefore we compared the female reproductive organ between *osabcg26* and the wild-type. SEM examination showed that the *osabcg26* and wild-type pistils were similar in morphology (Supplementary Fig. S4). Rice embryo sac development was divided into six stages from pre-meiosis to mature stage based on previous research [36]. Microscopic analysis indicated that the wild-type and *osabcg26* mutant exhibited no obvious difference in the ovary and embryo sac from pre-meiosis to mature stage (Supplementary Fig.

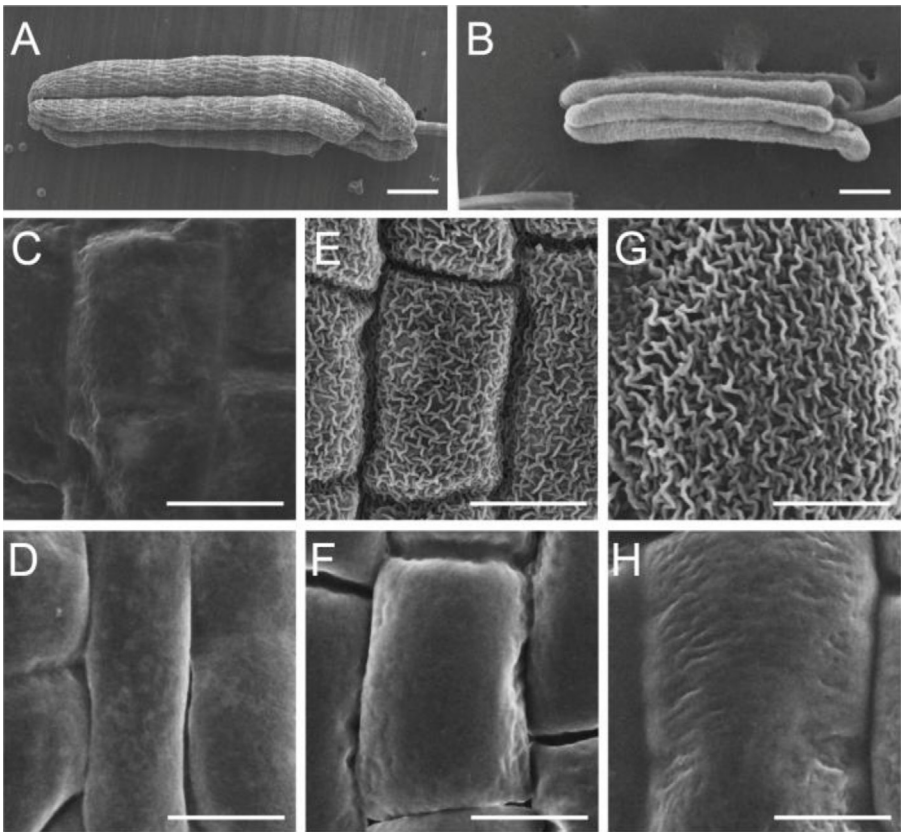

Fig. 4. SEM observation of the wild-type and *osabcg26* anther epidermis. (A, B) The anthers at stage 12. (C–H) Anther epidermis from stage 10–12. Wild-type anthers are shown in A, C, E, G, and *osabcg26* anthers are shown in B, D, F, H. Stage 10 (C, D), stage 11 (E, F) and stage 12 (G, H). Scale bars: A and B, 200 μm; C–H, 10 μm.

S5A-B). These results indicated that the *osabcg26* mutation did not significantly affect the morphological development of the pistil.

To further investigate the possible function of *OsABCG26* in the pistil, we pollinated the *osabcg26* stigma with wild-type pollen and then observed pollen germination and pollen tube growth in the pistil. In self-pollinated wild-type, pollen germinated on the stigma, and pollen tube grew to the ovule micropyle within 2 h after pollination (Fig. 8A–B). On the *osabcg26* stigma, the wild-type pollen germinated normally, but the pollen tube typically ceased growth within the upper region of the pistil and could not reach the micropyle for fertilization, even 8 h after pollination, resulting in low seed setting within the manually pollinated *osabcg26* (Fig. 8E–H, Supplementary Table S2-3). As a control, we examined pollen germination and pollen tube growth in the *osabcg15* mutant derived from HHZ. *osabcg15* has a point mutation in the 6th exon that causes an amino acid substitution at the 540 position from Asp (codon GAC) to Val (codon GTC) (data not shown). In contrast to *osabcg26* mutant, wild-type pollen germination and tube growth in the *osabcg15* pistil were similar to those in the wild-type plant, leading to high seed setting in the manually pollinated *osabcg15* mutant (Fig. 8I–L, Supplementary Table S2–3).

To verify that the defects of anther development and pollen tube growth in the *osabcg26* mutant was indeed caused by the mutation in *OsABCG26,* we created new mutations in *OsABCG26* in a *japonica* rice cultivar Wuyunjing7 using the CRISPR/Cas9 targeting system. Four independent homozygous lines were obtained that had mutations in two target sites, one in exon 2 and another in exon 3 of *OsABCG26* (Supplementary Fig. S6A–B). As expected, these mutants showed short whitish anthers lacking pollen grain (Supplementary Fig. S6C–D). After manual pollination with the wild-type pollens, all four mutants exhibited normal pollen germination but defective pollen tube growth within the pistil (Supplementary Fig. S6E–F), confirming the role of *OsABCG26* in pollen-pistil interactions.

Taken together, these results indicated that OsABCG26 plays an important role in pollen-pistil interactions by affecting pollen tube growth within the pistil.

4. Discussion

Wax, cutin and sporopollenin are essential components for the formation of anther cuticle and pollen exine, respectively. Their lipid precursors are synthesized by the secretory tapetal cells and transported to the anther and microspore surface for deposition. Several ABCG transporters, including *AtABCG11*, *AtABCG12*, *AtABCG26*, and *OsABCG15*, have been reported with a role in anther cuticle and pollen exine formation by regulating the transport of lipid precursors from the tapetum [11,13–20]. Mutations of these genes lead to male sterility. In this study, we identified a point mutation affecting the exon-intron splicing in *OsABCG26*, leading to male sterility in rice. *OsABCG26* was specifically expressed in the anther and pistil. Cytological analysis revealed that *osabcg26* mutant displayed defects in tapetal cells, Ubisch bodies, pollen exine, and anther cuticle. Furthermore, the expression levels of several key genes involved in lipid metabolism and transport were significantly altered in the *osabcg26* anther. Our findings suggested that, like the four published ABCG transporters, *OsABCG26* is required for normal formation of anther cuticle and pollen exine by regulating the transport of lipid precursors from the tapetum. Mutation of *OsABCG26* may disrupt the homeostasis of lipid metabolism in tapetum.

In addition to its role in anther development and pollen fertility, OsABCG26 also plays an important role in supporting pollen tube growth within the pistil. Previously, lipids have been demon-

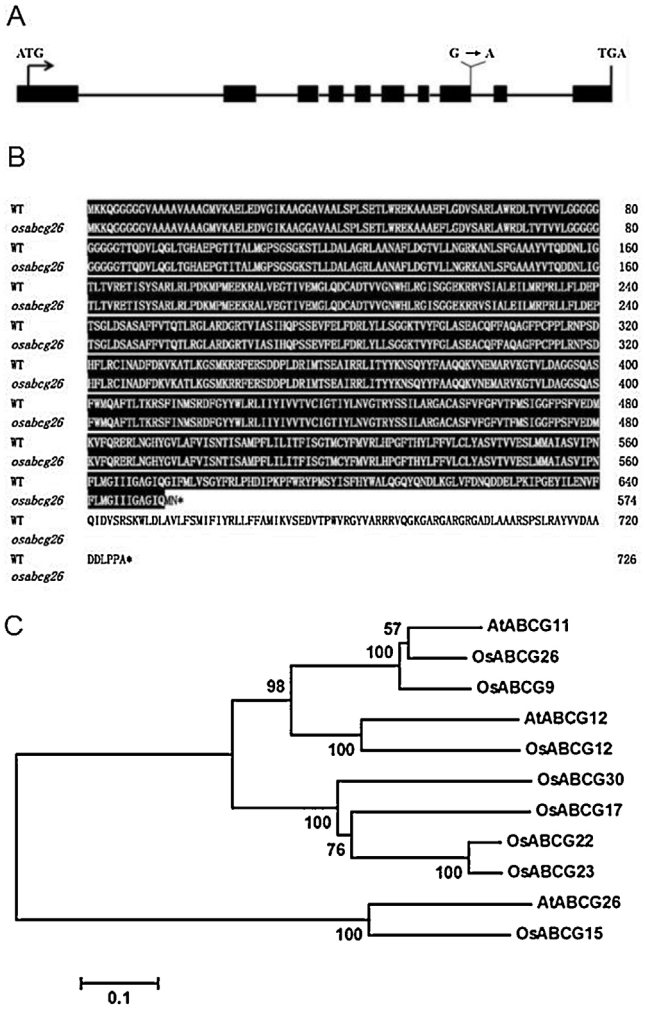

Fig. 5. Characterization of *OsABCG26*. (A) Wild type *OsABCG26* gene structure. Mutation of G to A in *osabcg26* is shown. Black box indicates exon and horizontal line indicates intron. (B) Amino acid sequence comparison of OsABCG26 in wild-type and *osabcg26* mutant. (C) Phylogenetic analysis of *OsABCG26* homologues in *Arabidopsis* and rice.

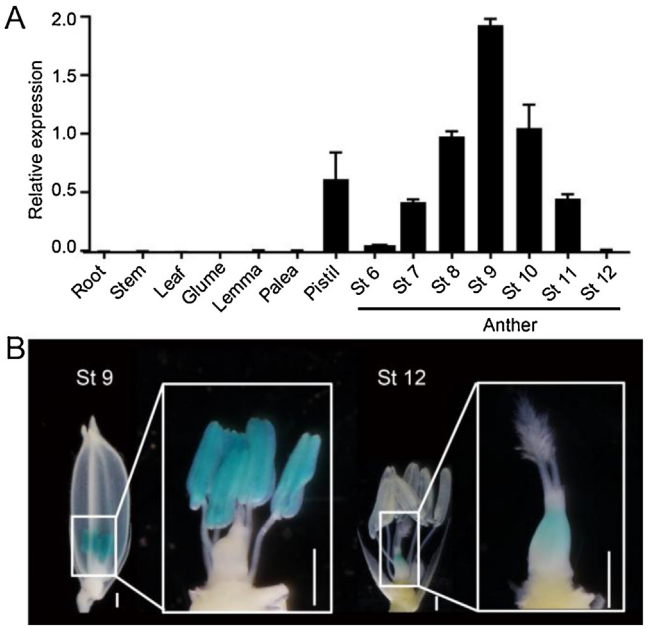

Fig. 6. The expression analysis of *OsABCG26*. (A) Relative expression of *OsABCG26* in various tissues. Anthers were collected at different developmental stages (St 6–12). Pistils and other tissues were harvested from plants with anther development at stage 12. The expression levels were determined by qRT-PCR. *OsACTIN1* was used as internal standards. Data are shown as means ± *SD* ($n = 3$). (B) GUS staining of the promoter-GUS transgenic plant. Gene specific expressions in anther and pistil are shown at anther development stage 9 and 12, respectively. Bar = 2 mm.

strated to be essential for normal pollen-stigma interaction in species such as *Arabidopsis* and *Brassica* [37–39]. Lipids presenting at the pollen-stigma interface are to establish a gradient of water potential between the pollen grain and the turgid cells of the stigma, which guides the germinating pollen to grow through the stigma [40]. *osabcg26* displayed normal pollen germination and pollen tube growth through the stigma, indicating that the *osabcg26* mutation does not affect stigma function. However, most of the wild-type pollen tubes ceased growth in the upper region of the *osabcg26* pistil, and only a few pollen tubes could reach the micropyle for fertilization. As a result, only a few seeds were produced. Yet the *OsABCG26/osabcg26* heterozygous plants exhibited normal seed setting and genotype segregation in Mendelian fashion in self-pollination progeny, indicating that the defect in pollen tube growth in *osabcg26* pistil was determined by the sporophyte, not by the gametophyte. Based on the function of OsABCG26 in the transport of lipid precursors, it is plausible to speculate that OsABCG26 may regulate lipid constituents or their distribution in the transmitting tissue of the pistil, which is required for normal growth of the pollen tube through the pistil. Further investigations are needed to decipher the mechanism of the pollen tube growth defect in the *osabcg26* pistil and to pinpoint the precise role of OsABCG26 in pollen-pistil interactions.

Prior to our manuscript submission, an allelic mutant of *OsABCG26* isolated from rice cultivar 9522 (*O. sativa* ssp. *japonica*) was reported to play a similar function in the formation of anther cuticle and pollen exine, but the function of OsABCG26 in pollen tube growth was not reported [29]. Compared with this study, we showed some unique properties of *OsABCG26* in rice cultivar HHZ (*O. sativa* ssp. *indica*). For example, the expression level of *OsABCG26* reached the maximum at stage 9 in our study, while at stage 10 in their study. The kinetic expression patterns of certain lipid metabolism or regulatory genes such as *CYP704B2*, *TDR* and *GAMYB* in both the wild-type and mutant anthers were different from those in their study. These inconsistencies between the two studies may potentially be due to the effect of the different genetic backgrounds.

Similar to most ABC transporters belonging to the G subfamily, OsABCG26 consists a nucleotide-binding domain (NBD) and an ABC2 transmembrane domain (TMD) (Supplementary Fig. S3). Mutation in *OsABCG26* resulted in a truncation in the TMD region. Although AtABCG11 is the closest homolog to OsABCG26 in the phylogeny (Fig. 5C), their expression patterns were quite different. *OsABCG26* is specifically expressed in reproductive tissues (Fig. 6A and B), whereas *AtABCG11* is expressed in both vegetative and reproductive tissues [13,14]. Additionally, *osabcg26* displayed defects in anther cuticle and pollen exine formation, whereas *atabcg11* showed defective cuticle formation in vegetative and reproductive tissues [13,14]. These differences between *OsABCG26* and *AtABCG11* suggested that the two ABCG transporters may have diverged in some of their functions during evolution.

Recently, four research groups reported that *OsABCG15* is involved in the transport of lipidic precursors for anther cuticle and pollen exine formation [17–20]. Morphological investigation of *osabcg26* demonstrated that *osabcg26* and *osabcg15* exhibited similar phenotypes during anther and pollen development. During early developmental stages, *osabcg26* displayed normal primary sporogenous cells and the four layers of the anther wall (Fig. 2A–D).

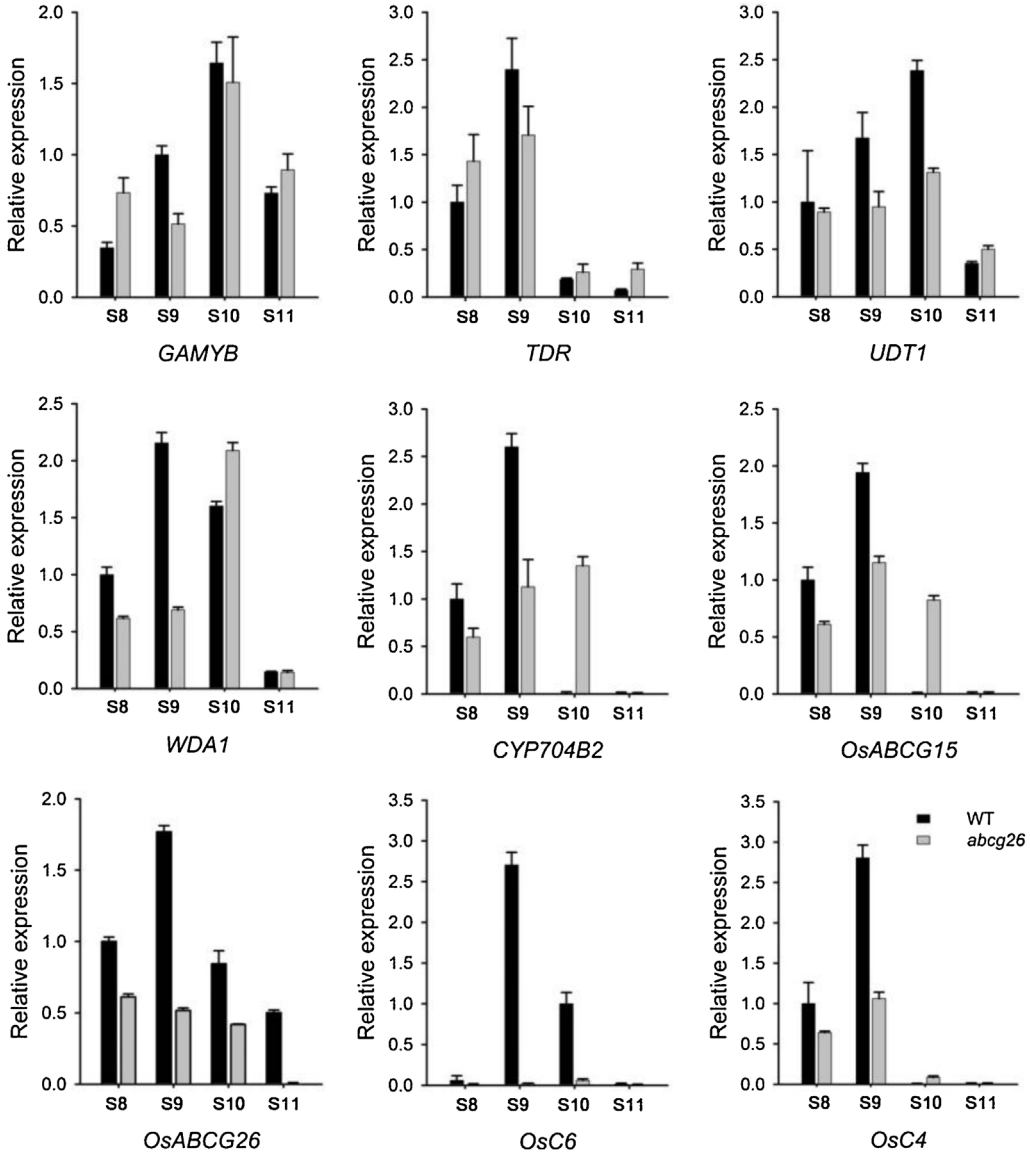

Fig. 7. Expression analysis of genes related to anther lipid metabolism and transport. Wild-type (WT) and *osabcg26* anthers at stages 8–11 (S8–S11) were collected for RNA extraction. Gene expression of *GAMYB*, *TDR*, *UDT1*, *WDA1*, *CYP704B2*, *OsABCG15*, *OsABCG26, OsC6* and *OsC4* was examined by qRT-PCR analysis. *OsACTIN1* was used as internal standard. Data are shown as means ± *SD* (*n* = 3).

However, after meiosis, the degeneration of the endothecium, the middle layer, and the tapetum was abnormal (Fig. 2E–N). In addition, *osabcg26* showed obvious defect in the formation of Ubisch bodies. Compared with the abundant Ubisch bodies presenting in the peripheral region of the wild-type tapetum, no Ubisch body was formed in mutant, leading to the defective anther cuticle and pollen exine and eventually microspore abortion (Fig. 3A–P). The expression patterns of *OsABCG15* and *OsABCG26* were similar [14–17]. Moreover, mutations of *OsABCG15* and *OsABCG26* both significantly reduced the expression of genes related to lipid metabolism and transport in anther, including *UDT1*, *WDA1*, *CYP704B2*, *OsC4*, OsC6, and *OsABCG15* [17–20]. These similarities suggested that *OsABCG15* and *OsABCG26* may cooperatively function in the formation of the anther cuticle and the pollen exine.

Both *OsABCG26* and *OsABCG15* encode a half-size ABCG transporter. The half-size ABCG transporter can form homodimers with itself or heterodimers with other half-size ABCG transporters to form a functional full-size transporter [41]. Thus, it is possible that OsABCG26 directly interacts with OsABCG15 to transport lipidic precursors in the rice anther. It is also possible that OsABCG26 and OsABCG15 both function in the form of homodimers, and each transports specific substrates required for anther cuticle and pollen exine formation. Analyses of *osabcg15 osabcg26* double mutant and localization of OsABCG15 and OsABCG26 in anthers also suggested that OsABCG26 may cooperate with OsABCG15 to regulate the formation of anther cuticle and pollen exine [29]. Future studies on the functional form of OsABCG26 and OsABCG15 *in vivo* are required to reveal how they regulate the transport of lipidic precursors in the rice anther.

Author contribution

Z.C., Z.C. and Y.W. performed most of the research; N.Y. supervised microscopic analyses; G.X., J.L., N.W., Q.L. and G.Y. participated in the characterization of the gene; X.T. designed and supervised the study; J.X. drafted the manuscript, J.X. and X.T. revised the manuscript. All of the authors discussed the results and commented on the manuscript.

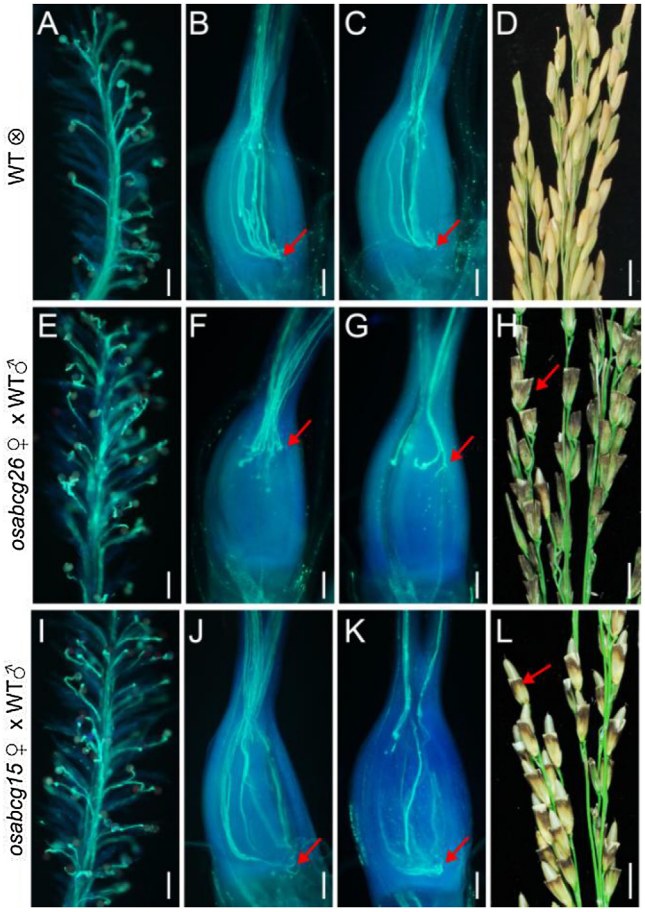

Fig. 8. Pollen tube growth and seed setting in WT, *osabcg26* and *osabcg15*. (A–D) pollen tube growth and seed setting in self-pollinated WT plant. (E–H) and (I–L), pollen tube growth and seed setting in *osabcg26* (E–H) and *osabcg15* (I–L) manually pollinated with WT pollen respectively. Pollen was stained with aniline blue at 30 min (A, E and I), 2 h (B, F, J) and 8 h (C, G, K) after pollination. Pollen germination in the stigma (A, E and I) and pollen tube growth in the ovary (B, C, F, G, J and K) were showed. Pollen tubes reached the micropylar region of the ovule in WT and *osabcg15* (B, C, J and K) but ceased growth at the top region of the ovary in *osabcg26* mutant (F, G). (D, H, L) showed seed setting in WT (D), *osabcg26* (H) and *osabcg15* (L). Arrows indicate excised husks in *osabcg26* (H) and *osabcg15* (L). Scale bars: A–C, E–G and I–K, 100 μm; D, H, and L, 5 mm. (For interpretation of the references to colour in this figure legend, the reader is referred to the web version of this article.)

Acknowledgments

We thank the Microscope Center in Sun Yat-Sen University for using their facilities for microscopic analysis. This work was supported by the National Natural Science Foundation of China (31560082), Guangdong Innovative Research Team Program (No. 201001S0104725509), the Ministry of Agriculture Transgenic Project (2012ZX08001001), and Shenzhen Commission on Innovation and Technology (JCYJ20140411140453785, CXZZ20140411140647863, JCYJ201304021545202). We are grateful to Roger Thimony for critical reading and editing of the manuscript.

Appendix A. Supplementary data

Supplementary data associated with this article can be found, in the online version, at http://dx.doi.org/10.1016/j.plantsci.2016.09.006.

References

[1] D. Zhang, X. Luo, L. Zhu, Cytological analysis and genetic control of rice anther development, J. Genet. Genom. 38 (2011) 379–390.
[2] J. Shi, M. Cui, L. Yang, Y.J. Kim, D. Zhang, Genetic and biochemical mechanisms of pollen wall development, Trends Plant Sci. 20 (2015) 741–753.
[3] L. Samuels, L. Kunst, R. Jetter, Sealing plant surfaces: cuticular wax formation by epidermal cells, Annu. Rev. Plant Biol. 59 (2008) 683–707.
[4] H. Li, D. Zhang, Biosynthesis of anther cuticle and pollen exine in rice, Plant Signal. Behav. 5 (2010) 1121–1123.
[5] L. Kunst, A.L. Samuels, Biosynthesis and secretion of plant cuticular wax, Prog. Lipid Res. 42 (2003) 51–80.
[6] W.J. Guilford, D.M. Schneider, J. Labovitz, S.J. Opella, High resolution solid state CNMR spectroscopy of sporopollenins from different plant taxa, Plant Physiol. 86 (1988) 134–136.
[7] R.J. Scott, M. Spielman, H.G. Dickinson, Stamen structure and function, Plant Cell 16 (Suppl) (2004) S46–S60.
[8] P. Piffanelli, J.H.E. Ross, D.J. Murphy, Biogenesis and function of the lipidic structures of pollen grains, Sex. Plant Reprod. 11 (1998) 65–80.
[9] T. Ariizumi, K. Toriyama, Genetic regulation of sporopollenin synthesis and pollen exine development, Annu. Rev. Plant Biol. 62 (2011) 437–460.
[10] J. Jiang, Z. Zhang, J. Cao, Pollen wall development: the associated enzymes and metabolic pathways, Plant Biol. 15 (2013) 249–263.
[11] G. Zhao, J. Shi, W. Lang, D. Zhang, ATP binding cassette G transporters and plant male reproduction, Plant Signal. Behav. 11 (2016) e1136764.
[12] J.A. Pighin, H. Zheng, L.J. Balakshin, I.P. Goodman, T.L. Western, R. Jetter, L. Kunst, A.L. Samuels, Plant cuticular lipid export requires an ABC transporter, Science 306 (2004) 702–704.
[13] D. Panikashvili, S. Savaldi-Goldstein, T. Mandel, T. Yifhar, R.B. Franke, R. Hofer, L. Schreiber, J. Chory, A. Aharoni, The *Arabidopsis DESPERADO/AtWBC11* transporter is required for cutin and wax secretion, Plant Physiol. 145 (2007) 1345–1360.
[14] T.D. Quilichini, M.C. Friedmann, A.L. Samuels, C.J. Douglas, *ATP-binding cassette transporter G26* is required for male fertility and pollen exine formation in *Arabidopsis*, Plant Physiol. 154 (2010) 678–690.
[15] H. Choi, J.Y. Jin, S. Choi, J.U. Hwang, Y.Y. Kim, M.C. Suh, Y. Lee, An ABCG/WBC-type ABC transporter is essential for transport of sporopollenin precursors for exine formation in developing pollen, Plant J. 65 (2011) 181–193.
[16] X.Y. Dou, K.Z. Yang, Y. Zhang, W. Wang, X.L. Liu, L.Q. Chen, X.Q. Zhang, D. Ye, WBC27, an adenosine tri-phosphate-binding cassette protein, controls pollen wall formation and patterning in *Arabidopsis*, J. Integr. Plant Biol. 53 (2011) 74–88.
[17] B.X. Niu, F.R. He, M. He, D. Ren, L.T. Chen, Y.G. Liu, The ATP-binding cassette transporter *OsABCG15* is required for anther development and pollen fertility in rice, J. Integr. Plant Biol. 55 (2013) 710–720.
[18] P. Qin, B. Tu, Y. Wang, L. Deng, T.D. Quilichini, T. Li, H. Wang, B. Ma, S. Li, *ABCG15* encodes an ABC transporter protein, and is essential for post-meiotic anther and pollen exine development in rice, Plant Cell Physiol. 54 (2013) 138–154.
[19] L. Zhu, J. Shi, G. Zhao, D. Zhang, W. Liang, *Post-meiotic deficient anther1 (PDA1)* encodes an ABC transporter required for the development of anther cuticle and pollen exine in rice, J. Plant Biol. 56 (2013) 59–68.
[20] L. Wu, Y. Guan, Z. Wu, K. Yang, J. Lv, R. Converse, Y. Huang, J. Mao, Y. Zhao, Z. Wang, H. Min, D. Kan, Y. Zhang, *OsABCG15* encodes a membrane protein that plays an important role in anther cuticle and pollen exine formation in rice, Plant Cell Rep. 33 (2014) 1881–1899.
[21] K.H. Jung, M.J. Han, D.Y. Lee, Y.S. Lee, L. Schreiber, R. Franke, A. Faust, A. Yephremov, H. Saedler, Y.W. Kim, I. Hwang, G. An, *Wax-deficient anther1* is involved in cuticle and wax production in rice anther walls and is required for pollen development, Plant Cell 18 (2006) 3015–3032.
[22] H. Li, F. Pinot, V. Sauveplane, D. Werck-Reichhart, P. Diehl, L. Schreiber, R. Franke, P. Zhang, L. Chen, Y. Gao, W. Liang, D. Zhang, Cytochrome P450 family member CYP704B2 catalyzes the ω-hydroxylation of fatty acids and is required for anther cutin biosynthesis and pollen exine formation in rice, Plant Cell 22 (2010) 173–190.
[23] J. Shi, H. Tan, X. Yu, Y. Liu, W. Liang, K. Ranathunge, R.B. Franke, L. Schreiber, Y. Wang, G. Kai, J. Shanklin, H. Ma, D. Zhang, *Defective Pollen Wall* is required for anther and microspore development in rice and encodes a fatty acyl carrier protein reductase, Plant Cell 23 (2011) 2225–2246.
[24] X. Yang, D. Wu, J. Shi, Y. He, F. Pinot, B. Grausem, C. Yin, L. Zhu, M. Chen, Z. Luo, W. Liang, D. Zhang, Rice *CYP703A3* a cytochrome P450 hydroxylase, is essential for development of anther cuticle and pollen exine, J. Integr. Plant Biol. 56 (2014) 979–994.
[25] D. Zhang, W. Liang, C. Yin, J. Zong, F. Gu, D. Zhang, *OsC6*, encoding a lipid transfer protein, is required for postmeiotic anther development in rice, Plant Physiol. 154 (2010) 149–162.
[26] K.H. Jung, M.J. Han, Y.S. Lee, Y.W. Kim, I. Hwang, M.J. Kim, Y.K. Kim, B.H. Nahm, G. An, Rice *Undeveloped Tapetum1* is a major regulator of early tapetum development, Plant Cell 17 (2005) 2705–2722.
[27] N. Li, D.S. Zhang, H.S. Liu, C.S. Yin, X.X. Li, W.Q. Liang, Z. Yuan, B. Xu, H.W. Chu, J. Wang, T.Q. Wen, H. Huang, D. Luo, H. Ma, D.B. Zhang, The rice *tapetum degeneration retardation* gene is required for tapetum degradation and anther development, Plant Cell 18 (2006) 2999–3014.

[28] K. Aya, M. Ueguchi-Tanaka, M. Kondo, K. Hamada, K. Yano, M. Nishimura, M. Matsuoka, Gibberellin modulates anther development in rice via the transcriptional regulation of GAMYB, Plant Cell 21 (2009) 1453–1472.
[29] G. Zhao, J. Shi, W. Liang, F. Xue, Q. Luo, L. Zhu, G. Qu, M. Chen, L. Schreiber, D. Zhang, Two ATP binding cassette G transporters rice *ATP binding cassette G26* and *ATP binding cassette G15*, collaboratively regulate rice male reproduction, Plant Physiol. 169 (2015) 2064–2079.
[30] Z. Chen, W. Yan, N. Wang, W. Zhang, G. Xie, J. Lu, Z. Jian, D. Liu, X. Tang, Cloning of a rice male sterility gene by a modified MutMap method, Yi Chuan 36 (2014) 85–93.
[31] S.O. Lochlainn, S. Amoah, N.S. Graham, K. Alamer, J.J. Rios, S. Kurup, A. Stoute, J.P. Hammond, L. Ostergaard, G.J. King, P.J. White, M.R. Broadley, High Resolution Melt (HRM) analysis is an efficient tool to genotype EMS mutants in complex crop genomes, Plant Methods 7 (2011) 43.
[32] X. Tang, A. Gomes, A. Bhatia, W.R. Woodson, Pistil-specific and ethylene-regulated expression of 1-aminocyclopropane-1-carboxylate oxidase genes in Petunia flowers, Plant Cell 6 (1994) 1227–1239.
[33] C. Wang, Y. Wang, Z. Cheng, Z. Zhao, J. Chen, P. Sheng, Y. Yu, W. Ma, E. Duan, F. Wu, L. Liu, R. Qin, X. Zhang, X. Guo, J. Wang, L. Jiang, J. Wan, The role of OsMSH4 in male and female gamete development in rice meiosis, J. Exp. Bot. 67 (2016) 1447–1459.
[34] N. Wang, H.J. Huang, S.T. Ren, J.J. Li, Y. Sun, D.Y. Sun, S.Q. Zhang, The rice wall-associated receptor-like kinase gene *OsDEES1* plays a role in female gametophyte development, Plant Physiol. 160 (2012) 696–707.
[35] X. Ma, Q. Zhang, Q. Zhu, W. Liu, Y. Che, R. Qiu, B. Wang, Z. Yang, H. Li, Y. Lin, Y. Xie, R. Shen, S. Chen, Z. Wang, Y. Chen, J. Guo, L. Chen, X. Zhao, Z. Dong, Y.G. Liu, A robust CRISPR/Cas9 system for convenient, high-efficiency multiplex genome editing in monocot and dicot plants, Mol. Plant 8 (2015) 1274–1284.
[36] T. Kubo, M. Fujita, H. Takahashi, M. Nakazono, N. Tsutsumi, N. Kurata, Transcriptome analysis of developing ovules in rice isolated by laser microdissection, Plant Cell Physiol. 54 (2013) 750–765.
[37] M. Wolters-Arts, W.M. Lush, C. Mariani, Lipids are required for directional pollen tube growth, Nature 392 (1998) 818–821.
[38] M. Wolters-Arts, L. Van der Weerd, A.C. Van Aeist, J. Van der Weerd, H. Van As, C. Mariani, Water conducting properties of lipids during pollen hydration, Plant Cell Environ. 25 (2002) 513–519.
[39] A.M. Sanchez, M. Bosch, M. Bots, J. Nieuwland, R. Feron, C. Mariani, Pistil factors controlling pollination, Plant Cell 16 (2004) S98–S106.
[40] W.M. Lush, T. Spurck, R. Joosten, Pollen tube guidance by the pistil of a Solanaceous plant, Ann. Bot. 85 (2000) 39–47.
[41] P.A. Rea, Plant ATP-binding cassette transporters, Annu. Rev. Plant Biol. 58 (2007) 347–375.